Molecular Therapy
Nucleic Acids
Original Article

Characterization of Circular RNAs in Vascular Smooth Muscle Cells with Vascular Calcification

Juhee Ryu,[1,2,3,4] Duk-Hwa Kwon,[1,4] Nakwon Choe,[1,4] Sera Shin,[1,4] Geon Jeong,[1,2,3] Yeong-Hwan Lim,[1,2,3] Jaetaek Kim,[5] Woo Jin Park,[1,6] Hyun Kook,[1,2,4] and Young-Kook Kim[1,2,3]

[1]Basic Research Laboratory for Vascular Remodeling, Chonnam National University Medical School, Jeollanam-do, Republic of Korea; [2]Department of Biomedical Sciences, Center for Creative Biomedical Scientists at Chonnam National University, Jeollanam-do, Republic of Korea; [3]Department of Biochemistry, Chonnam National University Medical School, Jeollanam-do, Republic of Korea; [4]Department of Pharmacology, Chonnam National University Medical School, Jeollanam-do, Republic of Korea; [5]Division of Endocrinology and Metabolism, Department of Internal Medicine, College of Medicine, Chung-Ang University, Seoul, Republic of Korea; [6]College of Life Sciences, Gwangju Institute of Science and Technology (GIST), Gwangju, Republic of Korea

Circular RNAs (circRNAs) are generally formed by back splicing and are expressed in various cells. Vascular calcification (VC), a common complication of chronic kidney disease (CKD), is often associated with cardiovascular disease. The relationship between circRNAs and VC has not yet been studied. Inorganic phosphate (Pi) was used to treat rat vascular smooth muscle cells to induce VC. circRNAs were identified by analyzing RNA sequencing (RNA-seq) data, and their expression change during VC was validated. The selected circRNAs, including circSamd4a, circSmoc1-1, circMettl9, and circUxs1, were resistant to RNase R digestion and mostly localized in the cytoplasm. While silencing circSamd4a promoted VC, overexpressing it reduced VC in calcium assay and Alizarin red S (ARS) staining. In addition, microRNA (miRNA) microarray, luciferase reporter assay, and calcium assay suggested that circSamd4a could act as a miRNA suppressor. Our data show that circSamd4a has an anti-calcification role by functioning as a miRNA sponge. Moreover, mRNAs that can interact with miRNAs were predicted from RNA-seq and bioinformatics analysis, and the circSamd4a-miRNA-mRNA axis involved in VC was verified by luciferase reporter assay and calcium assay. Since circSamd4a is conserved in humans, it can serve as a novel therapeutic target in resolving VC.

INTRODUCTION

Vascular calcification (VC) is one of the common complications in patients with chronic kidney disease (CKD). Traditional risk factors such as hypertension, diabetes, dyslipidemia, aging, and smoking are involved in the development of VC. There are two types of VC, atherosclerotic calcification and medial artery calcification; patients with CKD or diabetes typically present with medial artery calcification. Patients with CKD often demonstrate an elevated level of the calcium-phosphate product due to a decline in kidney function. The phosphate level is high, as it is not adequately secreted by the kidney, and phosphate absorption in the intestine and phosphate resorption in the bone are increased. The serum calcium level is raised due to increased calcium absorption in the gastrointestinal tract and calcium resorption in the bone. When this condition persists, it can cause VC in the vascular smooth muscle cells (VSMCs), which are the main component of the medial artery.[1,2] Although pharmacologic treatments such as phosphate binders, active vitamin D analog, and calcimimetics are available,[3] VC is still prevalent in patients with CKD.

Multiple mechanisms and factors affect VC. Since VC is commonly associated with cardiovascular disease (CVD), which is one of the leading causes of death around the world, exploring a new mechanism may be necessary to provide a novel insight into the pathogenesis of VC. While microRNAs (miRNAs) involved in VC have been already studied and have shown new insights into the development of VC,[3] the role of circular RNAs (circRNAs) remains unclear. circRNAs are one of the noncoding RNAs, which are generally formed by back-splicing events. They are mostly produced from the exon of the protein-coding gene, when the downstream 5′ splice site, which acts as a splice donor, binds to the upstream 3′ splice site, which serves as a splice acceptor. Because circRNAs do not have 5′ or 3′ ends, they are highly stable and generally resistant to exonuclease digestion.[4] circRNAs are known to function as a miRNA sponge, RNA-binding protein sponge, or regulator of transcription.[5–7] Some circRNAs have been recently revealed to be involved in translation.[8,9] circRNAs were considered as a byproduct of mRNA processing[10] and did not receive much attention previously. However, numerous RNA sequencing (RNA-seq) analyses demonstrated that the expression of circRNAs was quite prevalent in various tissues.[11] The expression of circRNAs has been extensively studied in neuronal cells;[12] however, detailed

Received 22 February 2019; accepted 5 November 2019;
https://doi.org/10.1016/j.omtn.2019.11.001.

Correspondence: Hyun Kook, Department of Pharmacology, Chonnam National University Medical School, Jeollanam-do, Republic of Korea.
E-mail: kookhyun@jnu.ac.kr
Correspondence: Young-Kook Kim, Department of Biochemistry, Chonnam National University Medical School, Jeollanam-do, Republic of Korea.
E-mail: ykk@jnu.ac.kr

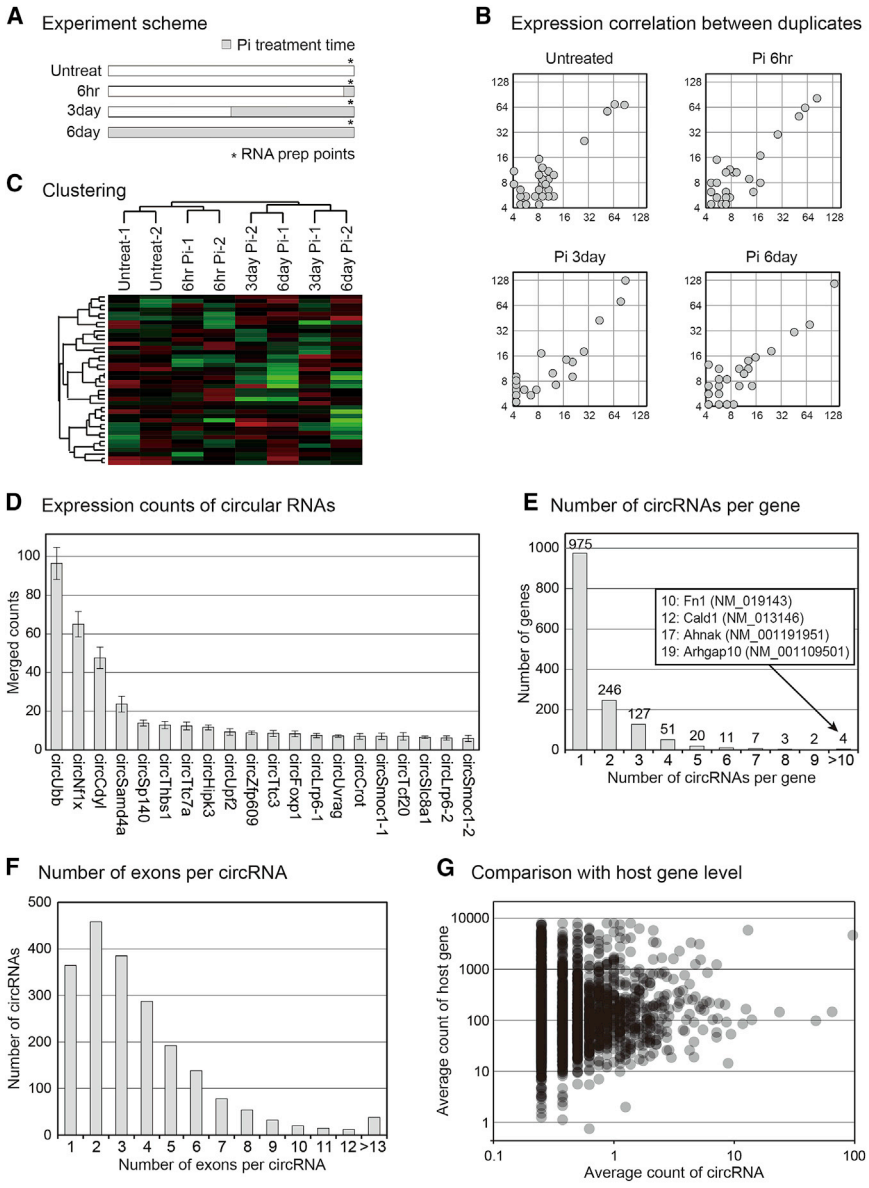

Figure 1. Identification of circRNAs in RVSMCs

(A) Experimental design of vascular calcification (VC) induction and RNA preparation. In primary RVSMCs, 2 mM inorganic phosphate (Pi) was treated for 6 h, 3 days, and 6 days, and RNA was prepared at the same time. (B) circRNA expression pattern in duplicates depending on Pi treatment time. Normalized circRNA counts from duplicate sets were used for depiction. (C) Heatmap of expression profile showing the unsupervised hierarchical clustering of circRNAs after VC induction. Color bars were used to indicate relative expression. (D) Highly expressed circRNAs in RVSMCs. Data are represented as mean ± SD. For circRNA annotation, when two different isoforms of circRNAs are generated from the same host gene—for example, the Smoc1 gene—they were designated accordingly, such as, in this case, circSmoc1-1 and circSmoc1-2, respectively. (E) The number of circRNAs generated from each gene locus. (F) Analysis of the number of exons constituting circRNAs. (G) Scatterplot showing the correlation of circRNA and its host gene expression. The average count of each circRNA and its host gene was used to depict the scatterplot.

studies in VSMCs are lacking.[13–16] Moreover, the relationship between circRNA expression and VC has not yet been elucidated. Therefore, we decided to investigate the role and regulation of circRNAs involved in VC in rat vascular smooth muscle cells (RVSMCs).

RESULTS

Identification and Characterization of circRNAs in VC

To characterize the circRNA expression changes during VC, inorganic phosphate (Pi) was used to treat RVSMCs at three different intervals: 6 h, 3 days, and 6 days. Simultaneously, a sample without Pi treatment was used as control (Figure 1A). To validate our cellular model of vascular calcification, we performed Alizarin red S (ARS) staining and qRT-PCR to observe the change of calcification depending on the duration of Pi treatment. ARS staining and expression of Bmp2 mRNA, a pro-calcifying factor, was enhanced by Pi treatment with time-dependent manner, validating our calcification model (Figure S1).

The RNA was extracted from these RVSMCs, and the transcriptome was analyzed by RNA sequencing. circRNAs were detected by using the DCC algorithm[17] with a STAR read mapper,[18] and back-splicing junctions were discovered (see Materials and Methods). We confirmed that circRNA expression shows a high correlation between duplicate samples for four different time points (Figure 1B). We also performed an unsupervised clustering based on the expression level of circRNAs and found that duplicates from each time point clustered together (Figure 1C). A full list of the 2,077 identified circRNAs, along with their expression levels in each sample, is included in Table S1. The top 20 circRNAs based on their expression levels in RVSMCs are summarized in Figure 1D. We named the circRNAs based on the host gene from which they were produced. For those gene loci where more than two different forms of circRNAs were generated, such as *Smoc1* gene locus, we designated their names as circSmoc1-1 and circSmoc1-2 (Figure 1D). We calculated the number of circRNAs generated from a single gene. Although the majority of genes produced one circRNA, in cases such as those of *Cald1*, *Ahnak*, and *Arhgap10* loci, more than 10 different circRNAs were generated (Figure 1E). Similarly, the number of exons constituting each circRNA was calculated, and it was found that most circRNAs were composed

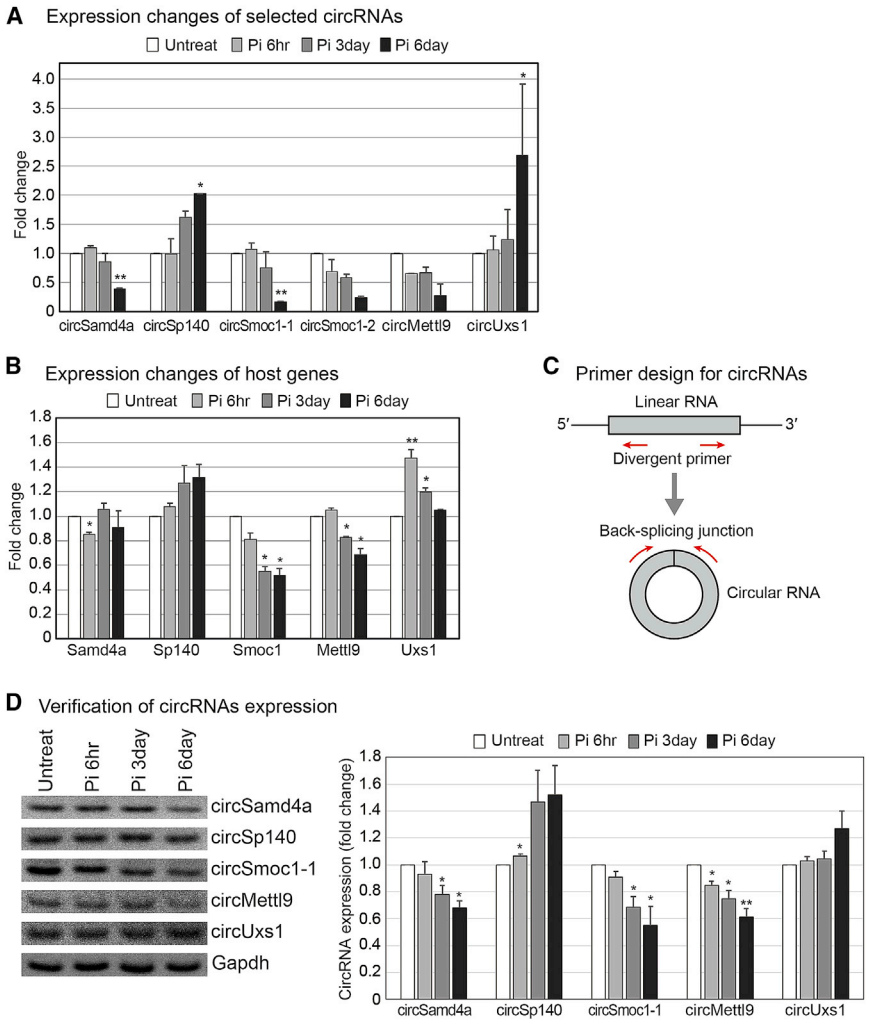

Figure 2. Regulation of circRNAs after VC

(A and B) Selected circRNA (A) and host gene (B) expression changes post-VC, depending on inorganic phosphate (Pi) treatment time (n = 2). In primary RVSMCs, 2 mM inorganic phosphate (Pi) was treated for 6 h, 3 days, and 6 days, respectively. Fold change of circRNA expression was calculated by using normalized circRNA expression counts in Table S1. (C) Illustration of the positions of PCR primers to amplify circRNAs. Divergent primers were designed to detect back-splicing junction of circRNAs. (D) Validation of circRNA expression post-VC induction by semiquantitative RT-PCR using divergent primers (n = 3). In primary RVSMCs, 2 mM Pi was treated for 6 h, 3 days, and 6 days, respectively. The expression of circRNAs was normalized to that of Gapdh. Data are displayed as mean ± SD. Student's t test was used for statistical analysis; *$p \leq 0.05$ versus untreated; **$p \leq 0.01$ versus untreated.

of 1–3 exons (Figure 1F). We also analyzed the relationship between circRNA expression and host gene expression (Figure 1G). As described in a previous report,[10] there was no specific correlation between circRNA and host gene levels, in general, for most circRNA-host gene pairs, indicating that their expressions were independent of each other.

Expression Change of circRNAs during VC

We found that the expressions of many circRNAs changed significantly after VC induction (Table S1). Among the identified circRNAs, six circRNAs with high average expression levels (normalized count > 5) and significant expression changes after VC (>2-fold change at any time point) were selected for further characterization. According to RNA sequencing data, circSp140 and circUxs1 were upregulated, while circSamd4a, circSmoc1-1, circSmoc1-2, and circMettl9 were downregulated after VC induction (Figure 2A). To investigate whether these circRNA expression changes have any correlation with host gene expression, we analyzed the host gene expression changes for these six circRNAs (Figure 2B). Three host genes, *Sp140* (SP140 nuclear body protein), *Smoc1* (secreted modular calcium binding protein 1), and *Mettl9* (methyltransferase like 9) showed expression patterns similar to those of the circRNAs produced from these loci, while *Samd4a* (sterile alpha motif domain containing 4A) and *Uxs1* (UDP-glucuronate decarboxylase 1) showed less correlation with their corresponding circRNAs. To verify the expression of circRNAs, divergent PCR primers were designed to amplify circSamd4a, circSp140, circSmoc1-1, circMettl9, and circUxs1 (Figure 2C). Between the two circRNAs generated from *Smoc1* locus, circSmoc1-1 was selected for further experimental validation, since its expression change after Pi treatment was more significant than that of circSmoc1-2 (Figure 2A). As seen in the PCR result, the circRNA expression showed a pattern similar to that of RNA sequencing data (Figure 2D; Figure S2A).

Characterization of Selected circRNAs

To investigate whether selected circRNAs indeed exist in a circular form, we tested the circular structure by treating the total RNAs from RVSMCs with RNase R, which degrades the linear RNAs. Most circRNAs were not affected by RNase R treatment, except circSp140, and were detected at their expected size (Figure 3A; Figure S2B). This result showed that the RNase R treatment can produce variable results depending on the circRNAs and that some circRNAs can be RNase R sensitive, as revealed in previous research.[19] Compared to circRNAs, linear RNA, such as the mRNA produced from the host gene of circSamd4a, and other mRNAs such as Gapdh and β-actin were completely degraded by RNase R treatment. The expected sequences near back-splice junctions of circRNAs, including circSamd4a, circSmoc1-1, circMettl9, and circUxs1, were confirmed by Sanger sequencing of the PCR products (Figure S2C).

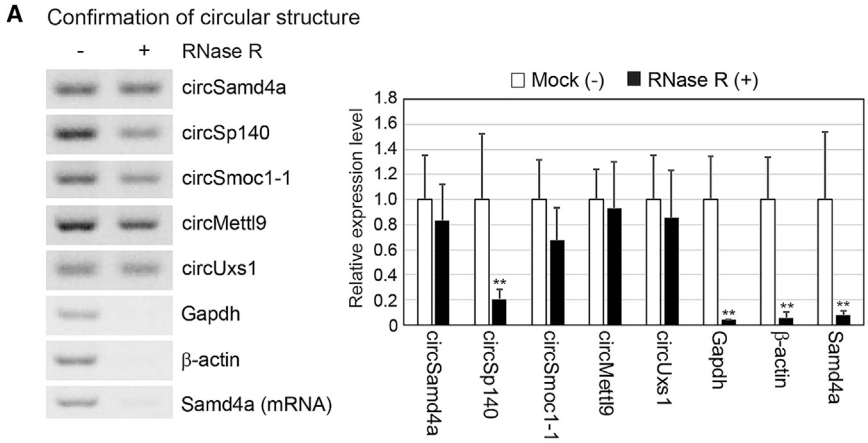

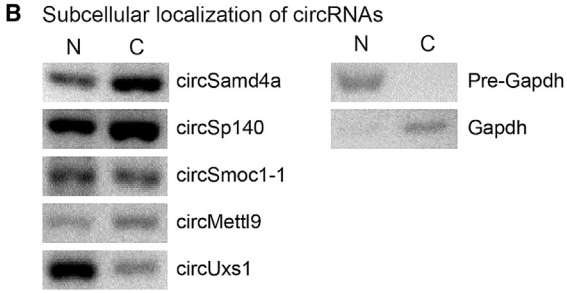

Figure 3. Characterization of Selected circRNAs

(A) Confirmation of the circular structure of circRNAs. circRNAs after RNase R treatment were quantified using RT-PCR (n = 3). RNase R was used to digest linear RNAs. The circRNAs were not affected, but the linear RNAs, including Gapdh, beta-actin, and host gene mRNA, were eliminated by RNase R treatment. The representative image for the quantification is included in Figure S2B. Student's t test was used for statistical analysis; $^{**}p \leq 0.01$ versus mock. (B) Subcellular localization of circRNAs. The cells were fractionated into nuclear and cytoplasmic fractions, and the expression of circRNAs was measured in each fraction. Pre-Gapdh was used as a control for nuclear RNA, and Gapdh was used as a control for cytoplasmic RNA.

The circRNAs are known to function in diverse cellular processes based on their localization. Therefore, we investigated the subcellular localization of circRNAs in the cells. From our subcellular fractionation experiment, it was revealed that most circRNAs were located in the cytoplasm (Figure 3B), suggesting that those cytoplasmic circRNAs may function as miRNA suppressors.[20] To study further the functional and mechanistic details of circRNAs as miRNA regulators, we selected circSamd4a, circSmoc1-1, and circMettl9. circUxs1 was localized mainly in the nucleus, and circSp140 was sensitive to RNase R treatment; hence, they were omitted from further study.

Cellular Function of circRNAs in VC

To investigate the function of circRNAs in VC, we decided to overexpress or silence circRNAs. Two small interfering RNAs (siRNAs) were designed for each circRNA to silence circRNA expression. The siRNAs were constructed around the back-splicing junction, as depicted in Figure 4A. Upon treating cells with siRNA, the expression of circRNAs decreased significantly (Figure 4B). We also tested whether the expression of host genes was altered by the siRNA treatment and found no significant change (Figure 4B). To test whether silencing circRNAs has any effect on VC, we performed calcium measurement assays. Only the knockdown of circSamd4a using two different siRNAs significantly increased calcium accumulation in the cells (Figure 4C). In addition, when the ARS staining was performed to verify the effect of circSamd4a knockdown, it was found that calcium accumulation was significantly increased (Figure 4D).

We also measured the level of VC-related marker genes after suppressing circSamd4a. We confirmed that the mRNA level of *Runx2* (Runt-related transcription factor 2) and *Alp* (Alkaline Phosphatase), the pro-calcification genes, and the protein level of Alp were significantly upregulated (Figures S3A and S3B). Since the knockdown of circSamd4a showed a significant change in calcium deposition and VC-related markers, we decided to investigate the overexpression effect only for this circRNA. In order to overexpress circSamd4a, a plasmid with the circularization sequences from *ZKSCAN1* gene[21] was used (Figure 4E). Compared with the control, circSamd4a overexpression vector increased the expression level of circSamd4a significantly (Figure 4E). The sequence of the circSamd4a overexpression product was confirmed by Sanger sequencing. To test whether circSamd4a overexpression has any effect on VC, calcium assay and ARS staining were performed, and VC-related marker genes were also measured. It was verified that calcium deposition (Figures 4F and 4G) and pro-calcification marker levels (Figures S3C and S3D) were significantly decreased by circSamd4a overexpression. These results suggest that circSamd4a is involved in VC.

Mechanism Study of circRNA as miRNA Sponge

Since we investigated the function of circSamd4a in VC and confirmed their cytoplasmic localization, we decided to explore whether circSamd4a can function as a miRNA sponge. Target miRNAs were predicted by selecting common candidates retrieved by two different bioinformatics databases, mirDB[22] and miRNA_targets.[23] The miRNA microarray was also performed to select the miRNAs that showed the expression change with anti-correlation compared to the expression change of circRNAs during VC (see Materials and Methods). From these analyses, three miRNA candidates that could interact with circSamd4a were selected (Figure 5A), and the base pairing between the target miRNAs, miR-125a-3p and miR-483-5p, and circSamd4a sequences was shown (Figure 5B). Since

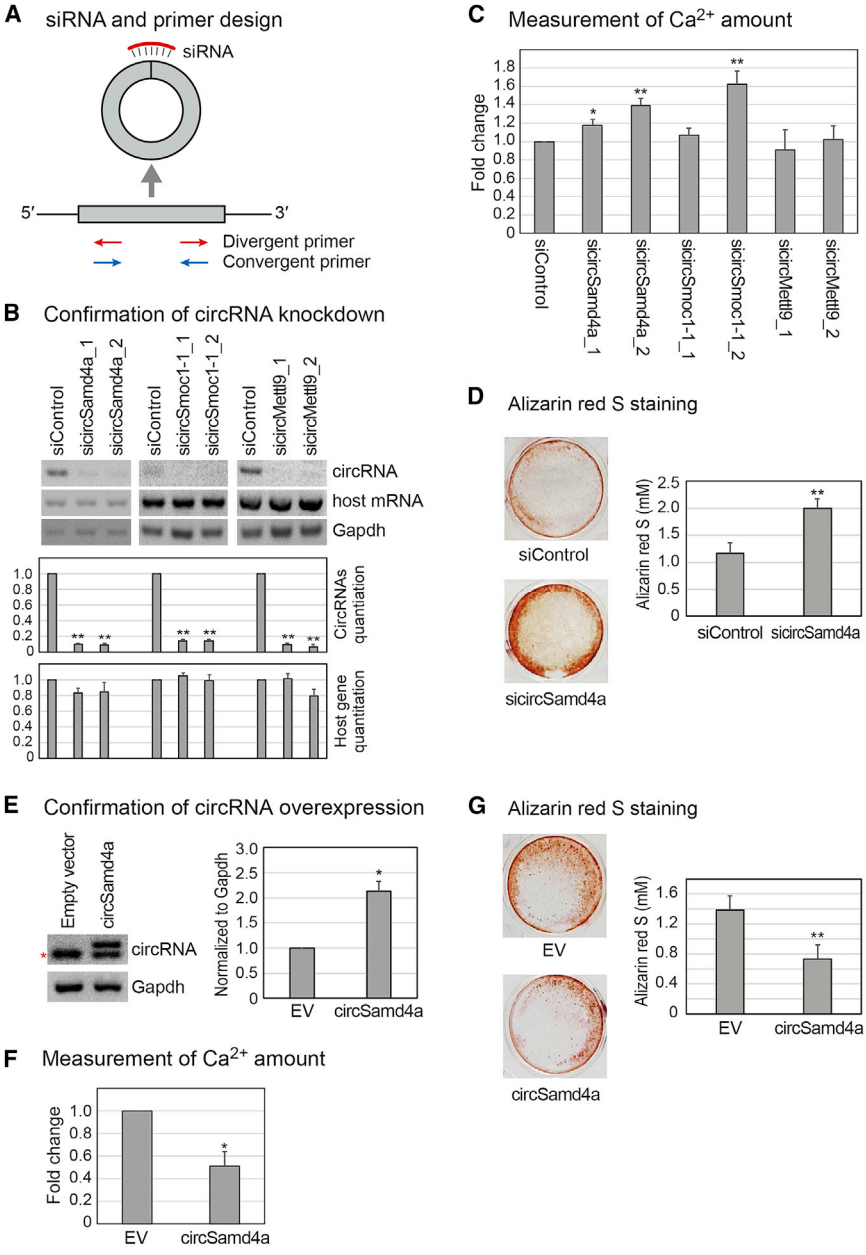

Figure 4. The Function of circRNAs in VC

(A) Diagram of PCR primers designed to amplify circRNA and host gene mRNA. circRNA expression was confirmed using divergent primers, whereas host gene mRNA expression was verified using convergent primers. (B) Expression of circRNAs and host gene mRNAs after knockdown of circRNAs in A10 cells using two different siRNAs. Expression was validated by semiquantitative RT-PCR (n = 3). The expression level was quantified and normalized to Gapdh mRNA. Data are displayed as mean ± SD. Student's t test was used for statistical analysis. **p ≤ 0.01 versus siControl. siControl, negative control siRNA. (C) Measurement of calcium content (milligrams of Ca/milligrams of protein) after knockdown of circRNAs (n = 5). In A10 cells, 1 day after the transfection, 2 mM inorganic phosphate (Pi) was treated for 3 days. Data are displayed as mean ± SD. Student's t test was used for statistical analysis. *p ≤ 0.05 versus siControl; **p ≤ 0.01 versus siControl. (D) Alizarin red S (ARS) staining after knockdown of circRNA. Calcium amounts were quantified by ARS staining (in millimolar) (n = 6). In A10 cells, 1 day after the transfection, 4 mM Pi was treated for 3 days. The representative photographs of cell culture dishes with ARS staining are shown. sicircSamd4a_2 was used to knock down circSamd4a. Data are displayed as mean ± SD. Student's t test was used for statistical analysis. **p ≤ 0.01 versus siControl. (E) Validation of circSamd4a overexpression after ectopic expression of circSamd4a-expressing vector in A10 cells (n = 3). The red star indicates the band of endogenous circRNA. Empty vector (EV) indicates Zkscan1 vector without insert, while circSamd4a refers to circSamd4a overexpression vector having the circSamd4a sequence within the Zkscan1 vector. Data are displayed as mean ± SD. Student's t test was used for statistical analysis. *p ≤ 0.05 versus EV. (F) Measurement of calcium content (milligrams of Ca/milligrams of protein) after the overexpression of circRNA (n = 3). In A10 cells, 1 day after the transfection, 2 mM Pi was treated for 3 days. Data are displayed as mean ± SD. Student's t test was used for statistical analysis; *p ≤ 0.05 versus EV. (G) ARS staining after the overexpression of circRNA. Calcium amounts were quantified by ARS staining (in millimolar) (n = 6). In A10 cells, 1 day after the transfection, 4 mM Pi was treated for 3 days. The representative photographs of cell culture dishes with ARS staining are shown. Data are displayed as mean ± SD. Student's t test was used for statistical analysis. **p ≤ 0.01 versus EV.

miR-99b-3p does not have a seed match region within circSamd4a, it was removed from further study. To validate whether circSamd4a can act as a miRNA sponge, luciferase reporter assays were conducted. When we inserted the circSamd4a sequences downstream of luciferase coding sequences and co-transfected this reporter with the targeting miRNA, luciferase activity was found to be significantly decreased compared to the control (Figure 5C). To confirm the role of miR-125a-3p and miR-483-5p in VC, a calcium assay was conducted. While calcium content was increased after adding either miR-125a-3p or miR-483-5p, it was decreased significantly when the miRNA was overexpressed together with circSamd4a (Figure 5D). These results suggest that there is a regulatory mechanism between the circSamd4a-miRNA pairs and that circSamd4a inhibits VC by acting as a miRNA sponge.

The Regulatory Relationship among circRNA, miRNA, and mRNA

Because miRNA can bind mRNA and influence its expression, we investigated potential mRNAs that can be regulated by the aforementioned selected miRNAs. We analyzed the candidate target mRNAs selected from bioinformatics databases mirDB[22] and Targetscan[24] and further narrowed down the list to only select the genes that

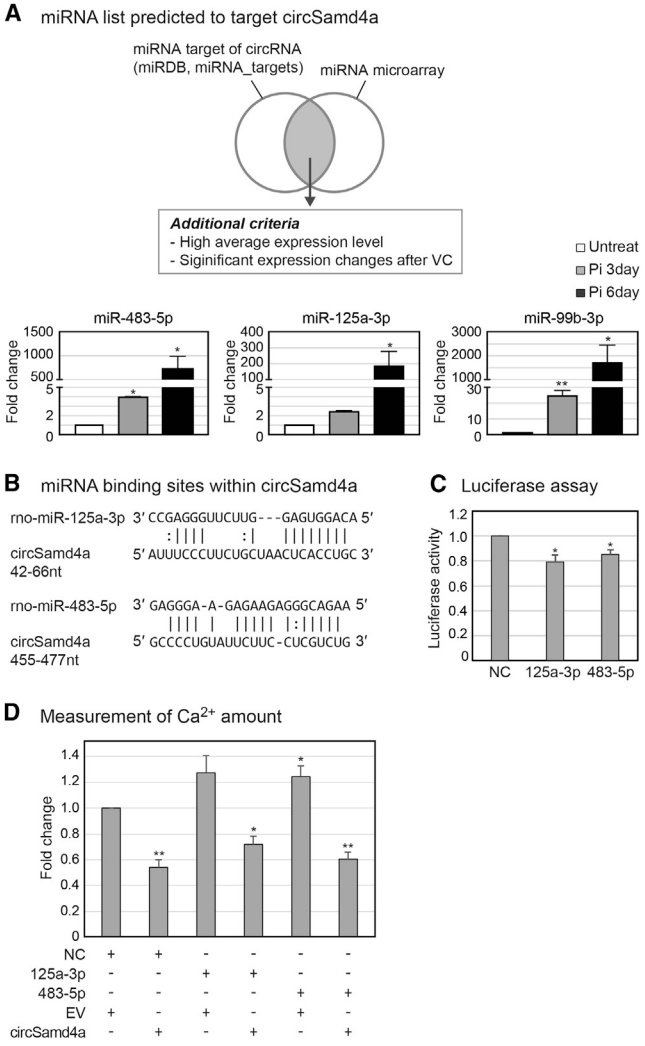

Figure 5. Mechanism of circSamd4a Acting as miRNA Sponge

(A) Analysis scheme to predict target miRNAs of circSamd4a. The expression change (fold change relative to untreated sample) of selected miRNAs during VC is shown (n = 2). Student's t test was used for statistical analysis. *p ≤ 0.05 versus untreated; **p ≤ 0.01 versus untreated. (B) Base pairing between the sequences of miRNAs and their binding sites within circSamd4a. (C) Validation of direct binding of miRNAs to circSamd4a by luciferase reporter assay (n = 4). Data are displayed as mean ± SD. Student's t test was used for statistical analysis. *p ≤ 0.05 versus NC. NC, negative control. (D) Measurement of calcium content (mg Ca/mg protein) after adding miRNAs (n = 3). In A10 cells, 1 day after the transfection, 2 mM inorganic phosphate (Pi) was treated for 3 days. Data are displayed as mean ± SD. Student's t test was used for statistical analysis. *p ≤ 0.05 versus NC+EV; **p ≤ 0.01 versus NC+EV. NC, negative control siRNA; EV, empty Zkscan1 vector without insert.

were related to calcium modulation, vasculature, or smooth muscle cells. Because the target mRNA expression change would typically have a negative correlation with miRNAs during VC, mRNAs—which were downregulated during VC based on RNA sequencing data—were selected as final candidates (Figure 6A). Calmodulin-regulated spectrin-associated protein family member 2 (Camsap2) was predicted to interact with both miR-125a-3p and miR-483-5p. Additionally, filamin A (Flna) was predicted to bind with miR-125a-3p. Sequences of miRNA binding sites within target mRNAs are shown in Figure 6B. To confirm whether the circSamd4a-miRNA-mRNA axis exists, luciferase reporter assays were conducted. When we inserted the 3′ UTR sequences of Camsap2 or Flna downstream of luciferase coding sequences and co-transfected the reporter with each targeting miRNA, luciferase activity was found to be significantly decreased compared to that of the control. When circSamd4a overexpression vector was added, however, the luciferase activity was fully recovered (Figure 6C). Furthermore, to confirm the effect of Camsap2 and Flna in VC, we performed a calcium assay. When Camsap2 or Flna expression was inhibited by siRNA, calcium deposition was increased. However, when circSamd4a overexpression vector was added along with the siRNA of Camsap2 or Flna, calcium content was decreased significantly (Figure 6D). These results suggest that there is a regulatory mechanism involved in the circSamd4a-miRNA-mRNA axis in vascular calcification.

DISCUSSION

To the best of our knowledge, this is the first study that identified and analyzed circRNA expression in VSMCs with VC. This study demonstrated that many circRNAs are highly expressed in RVSMCs (Figure 1). The six circRNAs—circSamd4a, circSp140, circSmoc1-1, circSmoc1-2, circMettl9, and circUxs1—were robustly expressed and showed differential regulation in RVSMCs with VC (Figure 2). Although there are several studies that demonstrated the existence of these circRNAs in human and mouse cells,[25–28] their function has not yet been studied. In this study, the existence of circSamd4a in RVSMCs and their biological roles were revealed for the first time. As shown from the calcium measurement, ARS staining and VC-related marker levels, silencing circSamd4a increased VC (Figures 4C and 4D; Figures S3A and S3B). On the contrary, when circSamd4a was overexpressed, VC was reduced, which implies that circSamd4a has an anti-calcification function (Figures 4F and 4G; Figures S3C and S3D). Since reducing VC is critical in patients with CKD and CVD, overexpression of circSamd4a may protect vascular smooth muscles and inhibit the progression of VC. This finding provides a novel insight for understanding the mechanism involved in the development of VC. Moreover, circSamd4a can be an important therapeutic target for VC.

Upon subcellular fractionation, circSamd4a was shown to be predominantly located in the cytoplasm (Figure 3B), which suggests that this circRNA may act as a miRNA sponge. The miRNA microarray data were used to select target miRNAs having a expression pattern negatively correlated with that of circSamd4a during VC (Figure 5A). The predicted targets, miR-125a-3p and miR-483-5p, were confirmed by luciferase reporter assay, suggesting that target miRNAs bind directly to circSamd4a (Figure 5C). The relationship of miRNAs and circSamd4a in VC was verified by the calcium assay, which showed that calcium deposition was increased after adding miRNAs, while calcium amount was reduced when circSamd4a was overexpressed (Figure 5D). This result further supported that circSamd4a plays a role as a miRNA sponge. Additionally, Camsap2, target mRNA of miR-125a-3p and

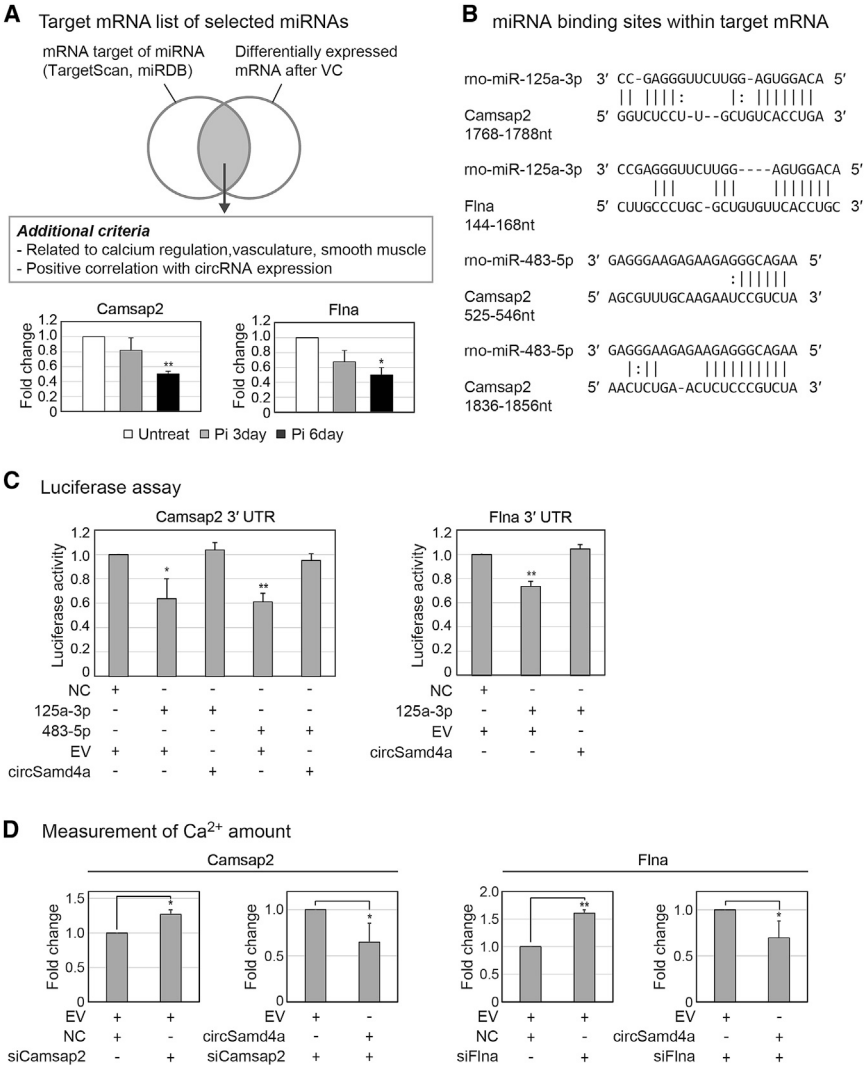

Figure 6. Relationship between circSamd4a, miRNA, and mRNA in VC

(A) Analysis scheme to predict the target mRNAs of selected miRNAs. The expression change (fold change relative to untreated sample) of each target mRNA during VC was measured from RNA sequencing data. Data are displayed as mean ± SD. Student's t test was used for statistical analysis; *p ≤ 0.05 versus untreated; **p ≤ 0.01 versus untreated. (B) Base pairing between the sequences of miRNAs and their binding sites within target mRNAs. (C) Confirmation of circSamd4a-miRNA-mRNA regulatory mechanism by luciferase reporter assay (Camsap2 3′ UTR, n = 4; Flna 3′ UTR, n = 3). Data are displayed as mean ± SD. Student's t test was used for statistical analysis; *p ≤ 0.05 versus NC+EV; **p ≤ 0.01 versus NC+EV. NC, negative control siRNA; EV, empty Zkscan1 vector without insert. (D) Measurement of calcium content (milligrams of Ca/milligrams of protein) after knockdown of mRNAs (n = 3). In A10 cells, 1 day after the transfection, 2 mM inorganic phosphate (Pi) was treated for 3 days. Data are displayed as mean ± SD. Student's t test was used for statistical analysis. *p ≤ 0.05; **p ≤ 0.01.

miR-483-5p, was expressed in smooth muscle cells and reported as the gene identified in coronary artery disease regions.[29] Moreover, It was found to be critical in vessel development in endothelial cells,[30] which is the source of osteoprogenitor cells in VC[31] and can promote VC in VSMC.[32] Flna, target mRNA of miR-125a-3p, interacts with P2Y2 nucleotide receptor, which regulates proliferation and migration of VSMC.[33] The P2Y2 nucleotide receptor was revealed to act as an inhibitor of VC.[34] To detect the relationship among circSamd4a, miRNA, and mRNA, a luciferase assay was performed. Luciferase activity was decreased when miRNA was added, but this effect was rescued when circSamd4a was also overexpressed. To investigate the roles of Camsap2 and Flna in VC, these mRNAs were suppressed by using siRNAs. Knockdown of these genes increased calcium deposition, confirming their roles in VC. However, calcium content was decreased in the Camsap2- or Flna-depleted sample when circSamd4a was overexpressed, which could compromise the effect of miRNAs (Figure 6D). Therefore, there can be a circSamd4a-miRNA-mRNA axis involved in the pathophysiology of VC. circSamd4a may regulate Camsap2 and Flna by acting as a sponge of miR-125a-3p and miR-483-5p. In addition, to investigate the possible protein-coding potential of circSamd4a, we utilized the bioinformatics database circRNADb[35] and found that circSamd4a has low protein-coding potential (Table S2). However, since circRNA can have other functions, such as protein sponge, further investigations are needed to elucidate the detailed mechanism of circSamd4a in VC.

Although expression of most circRNAs did not show significant correlation with host gene expression (Figure 1G), host genes of several circRNAs, such as circSp140, circSmoc1, and circMettl9, had expression changes similar to that of respective circRNAs (Figure 2). This suggests that there may be a transcriptional or post-transcriptional mechanism, which needs to be investigated in order to clarify the positive correlation between these circRNAs and their corresponding host genes.

Importantly, circSamd4a is conserved in human and mouse and is generated from the same corresponding exons in both the species (Figure S4A). The expression of circSamd4a was confirmed in human coronary artery smooth muscle cells (Figure S4B). Therefore, circSamd4a can be studied in human to test whether it can be used as a biomarker for diagnosis. In addition, *in vivo* effects of circSamd4a can be explored using model organisms such as mouse or rat.

From recent studies, it has been demonstrated that noncoding RNAs play important roles and may serve as critical therapeutic targets in

various diseases. Discovering noncoding RNAs, such as circRNAs, involved in VC can be a new approach to resolve VC. We found that circSamd4a plays important roles in regulating VC and that the modulation of this circRNA may serve as a novel therapeutic approach.

MATERIALS AND METHODS

Cell Culture

Primary RVSMCs were extracted from 6-week-old Sprague-Dawley rats and cultured in DMEM (high glucose; WELGENE) with 10% HyClone Fetal Bovine Serum (GE Healthcare Life Sciences). Cells were cultured from the third to the seventh passage and divided into four 100-mm dishes (Eppendorf). To induce VC, 2 mM Pi (pH 7.4) (Sigma) was used to treat RVSMCs for 6 h, 3 days, or 6 days in four different dishes, as published previously.[36] The RNAs of all samples were isolated simultaneously. A cell line of RVSMCs, A10 cells (CRL-1476, ATCC), were cultured using DMEM, high glucose, with 10% fetal bovine serum (WELGENE) for transfection and calcium assay. The HCT-116 cells were cultured using McCoy's 5A media (WELGENE) with 10% HyClone Fetal Bovine Serum (GE Healthcare Life Sciences) to perform luciferase reporter assay. Human coronary artery smooth muscle cells (Thermo Fisher Scientific) were cultured up to 4–8 passages using Medium 231 supplemented with Smooth Muscle Growth Supplement or Smooth Muscle Differentiation Supplement.

RNA Isolation and RNA-Seq Analysis

Total RNA was isolated using TRIzol Reagent (Thermo Fisher Scientific) as described in the manufacturer's protocol. DNase I (Takara) was used to remove residual DNA in RNA samples. RNA integrity was confirmed using Bioanalyzer (Agilent). The Ribo-Zero Gold rRNA Removal Kit (Illumina) was used to remove rRNA, and the TruSeq Stranded Total RNA Kit (Illumina) was used for the construction of the RNA sequencing library. The library was sequenced by HiSeq 2500 (Illumina) in the paired-end mode with 100 sequencing cycles.

Identification and Quantification of circRNAs

After removing the low-quality sequencing reads with Trimmomatic,[37] the expression levels of circRNAs were calculated using the STAR aligner[18] and DCC algorithm.[17] After combining the circRNA counts from duplicate samples, their expression was normalized using the total counts of circRNAs in each sample.

RNase R Digestion

To remove linear RNAs, the RNA samples were mixed with RNase R (Epicenter) and 10× RNase R buffer, while the control samples were incubated only with buffer. RNase R digestion was performed at 37°C for 20 min and inactivated at 95°C for 3 min.

Cell Fractionation

Cell fractionation was performed using the method modified from previously published reports.[38,39] The A10 cells, cultured in a 100-mm dish, were washed with PBS twice and collected by a scrapper. Cell pellets were mixed with 200 μL cold lysis buffer (20 mM HEPES [pH 7.4], 1 mM EDTA, 250 mM sucrose, 1 mM DTT) and were incubated on ice for 25 min. Then, 5 μL 10% NP-40 was added, and the mixture was incubated on ice for an additional 2 min. Lysates were centrifuged at 2,000 × *g* for 20 min at 4°C. Subsequently, the supernatant containing cytoplasmic fraction was centrifuged at 18,000 × *g* for 20 min at 4°C to remove the plasma membrane fraction, and the resulting supernatant was treated with TRIzol LS (Thermo Fisher Scientific) for RNA isolation. On the other hand, the pellet containing nuclear fraction was resuspended in K100 buffer D (20 mM Tris [pH 8.0], 100 mM KCl, 0.2 mM EDTA) and centrifuged again at 10,000 rpm for 5 min at 4°C, and the resulting pellet was treated with TRIzol to extract the nuclear RNA.

cDNA Synthesis and PCR

For each sample, the equal amount of RNA was reverse-transcribed using random hexamer (Thermo Scientific) and RevertAid reverse transcriptase (Thermo Scientific) to generate cDNA. A semiquantitative PCR was performed using forward and reverse primers designed for each circRNA using Phusion High-Fidelity DNA Polymerase (Thermo Scientific) in the Mastercycler Nexus X2 (Eppendorf). Results of semiquantitative PCR from gel electrophoresis were analyzed by using ImageJ (https://imagej.nih.gov/ij/),[40] and the expression of circRNA or mRNA was normalized by the expression of a control gene, Gapdh. For qRT-PCR, the Power SYBR Green Master Mix (Applied Biosystems) was used, and the reaction was conducted in Rotor-Gene Q (QIAGEN). circRNA and mRNA expression levels were normalized by that of Gapdh using the $2^{-\Delta Ct}$ method. The primer sequences are listed in Table S3.

Cloning of circRNA

To construct circRNA overexpression vectors, full sequences of circRNAs were amplified by using forward and reverse primers. The primer sequences are listed in Table S3. The primers included the nucleotides of the exon in circRNA, restriction enzyme site, and vector sequence. The pcDNA3.1(+) Zkscan1 MCS exon vector (Addgene, plasmid #69901), which was a gift from Jeremy Wilusz, was used for overexpression of circSamd4a. The vectors were digested and ligated with the PCR product using the EZ-Fusion Cloning Kit (Enzynomics), as per the manufacturer's instructions. After cloning, sequences of circSamd4a in Zkscan1 vector were confirmed by Sanger sequencing.

siRNA Construction

The siDesign center in Horizon Discovery (https://horizondiscovery.com/en/products/tools/siDESIGN-Center) or i-Score designer (https://www.med.nagoya-u.ac.jp/neurogenetics/i_Score/i_score.html)[41] were used to design siRNAs for each circRNA at the head-to-tail junctions and siRNAs for Camsap2 and Flna. If the 5′ end of antisense strand had equal or more hydrogen bonding than sense strand, the sense strand was modified so that the antisense strand can remain in RNA-induced silencing complex (RISC).[42] Designed siRNAs were tested for the presence of an internal secondary structure utilizing the OligoCalc (http://biotools.nubic.northwestern.edu/OligoCalc.html)[43]

and were selected if they did not make a secondary structure. The siRNAs were synthesized by Bioneer.

Transfection

For circRNA overexpression, 3.5×10^5 A10 cells were seeded in 60-mm dishes. One day later, 2.5 μg Zkscan1 vector containing circSamd4a was transfected using Lipofectamine 3000 (Invitrogen), as per the manufacturer's protocol. For the siRNA transfection experiment to suppress circRNAs, 2×10^5 A10 cells were seeded in 60-mm dishes. The siRNA was transfected into the cells at a final concentration of 30 nM using Lipofectamine 3000 a day after cell seeding. As negative control, AccuTarget Negative Control siRNAs (Bioneer) were used. The sequences of siRNAs are listed in Table S3.

Calcium Measurement Assay

For the calcium measurement experiment after circRNA overexpression, 3.5×10^4 cells were seeded in triplicate in 24-well plates. After a day, 0.25 μg Zkscan1 vector, with or without circSamd4a, was transfected into the cells. For the experiment after siRNA transfection, 2×10^4 cells were seeded in triplicate in 24-well plates. After a day, siRNA was transfected into the cells at a final concentration of 30 nM.

To test the effects of selected miRNAs in VC, 3.5×10^4 cells were seeded in triplicate in 24-well plates, and on the following day, either rno-miR-125a-3p miRNA mimic (MSY0004729, QIAGEN) or rno-miR-483-5p mimic (MSY0017201, QIAGEN) were co-transfected along with 0.25 μg Zkscan1 vector, with or without circSamd4a, at a final concentration of 20 nM. As a negative control, AllStars Negative Control siRNA (QIAGEN) was used.

To evaluate the role of target mRNAs in VC, 3.5×10^4 cells were seeded in triplicates in 24-well plates, and on the following day, either Camsap2 siRNA at a final concentration of 10 nM or Flna siRNA at a final concentration of 20 nM was co-transfected along with 0.25 μg Zkscan1 vector with or without circSamd4a. As a negative control, AccuTarget Negative Control siRNAs (Bioneer) were used.

Transfection agent used for all calcium assays was Lipofectamine 3000. The following day after transfection, 2 mM Pi was added for 3 days in treated samples, while normal media was used in control samples. Then cells were washed with 1× PBS and incubated with HCl (0.6 mol/L) overnight at 4°C. Calcium content was measured on the following day using a QuantiChrom Calcium Assay Kit (BioAssay Systems), and protein concentration for normalization was measured by using Bio-Rad Protein Assay Dye Reagent Concentrate as per the manufacturer's protocol.

ARS and Quantification

For the validation of the VC cellular model, primary RVSMCs were seeded in a 12-well plate. When cells reached about 80% confluence, 2 mM Pi was treated for 6 h, 3 days, and 6 days, respectively. For the confirmation of the effects of circSamd4a knockdown or its overexpression, A10 cells were seeded in a 24-well plate. After a day, cells were treated with either siRNA or overexpression vector. Then, 4 mM Pi was treated for an additional 3 days. For the ARS staining, cells were washed with PBS and fixed with 10% formalin at room temperature for 1 h. After removing 10% formalin, cells were washed three times with distilled water. When the samples were exposed to air and dried, 40 mM ARS solution (pH 4.2) (Sigma) was treated, and the samples were incubated overnight with rotation at room temperature. After removing the ARS solution, samples were washed with distilled water and PBS.

For ARS staining quantification, 300 μL 10% cetylpyridinium chloride (Sigma) was added to samples and incubated for 30 min. Then 200 μL dissolved solution was used to measure their absorbance at 562 nm by utilizing a microplate spectrophotometer (BioTek Instruments).

Western Blot Analysis

A10 cells were transfected with siRNA or plasmid, and 1 day later, 2 mM Pi was treated for 3 days. On the following day, cells were collected by trypsinization, and protein was extracted using ice-cold RIPA buffer (Biosesang). Protein content was quantified using the Pierce BCA Assay Kit (Thermo Fisher Scientific), and 20 μg protein was separated on 10% SDS-polyacrylamide gel. The protein was transferred onto methanol-activated polyvinylidene difluoride (PVDF) membrane (Millipore) and blocked with 5% skim milk (BD Biosciences) in 1× TBS-T (Tris-buffered saline, 0.1% Tween 20). Membrane was incubated with primary antibody overnight at 4°C. Then after washing with 1× TBS-T three times, it was incubated with secondary antibody for 1 h at room temperature. The blot was visualized using Immobilon Western Chemiluminescent HRP Substrate (Millipore) and Fusion Fx (Vilber). The primary antibody used was anti-Alp antibody (ab108337, Abcam) and anti-Actin antibody (a2066, Sigma-Aldrich) with a 1:1,000 dilution, and the secondary antibody used was anti-rabbit immunoglobulin G (IgG), horseradish peroxidase (HRP)-linked antibody (7074, Cell Signaling Technology) with a 1:5,000 dilution. Results of western blots were analyzed by using ImageJ (https://imagej.nih.gov/ij/),[40] and the expression of Alp was normalized by the expression level of a control gene, Actin.

miRNA Prediction

In order to predict miRNAs that can potentially interact with circRNA, bioinformatics databases such as miRDB (http://mirdb.org/index.html)[22] and miRNA_targets [23] were used. In bioinformatics databases, target miRNAs were predicted by using the mRNA target sequence. After retrieving the list of miRNAs that have binding sites in circRNAs, the expression of these miRNAs was analyzed by miRNA microarray, using the VC samples with calcification induced by treatment of RVSMCs with Pi for 3 or 6 days (unpublished data). The miRNAs with high average expression levels (raw average expression level $\geq$ 50) and significant expression changes after VC formation ($\geq$4-fold increase or decrease on day 6 compared to untreated sample) were selected as final candidates.

mRNA Prediction

To discover mRNAs that can potentially interact with miRNAs, bioinformatics databases, such as miRDB (http://mirdb.org/index.html)[22] and TargetScan (http://targetscan.org/vert_72/)[24] were used. Target mRNAs were predicted by using the miRNA sequence or miRNA name. After retrieving a list of mRNAs that might bind to miRNAs, mRNAs related to calcium regulation or smooth muscle cells were selected. The mRNA expression was analyzed by using RNA sequencing data, and only mRNAs having a negative correlation with miRNA in their expression change during VC (decreased more than 20% on day 6 after the induction of VC compared to an untreated sample) were selected as final targets.

Luciferase Reporter Assay

Luciferase reporter pGL3UC vector, which was constructed by inserting CMV promoter sequences and multiple cloning sites into pGL3 Basic (Promega), was used. To detect the interaction between circSamd4a and miRNAs, the sequence of circSamd4a was cloned into the multiple cloning sites at the 3′ UTR of pGL3UC. A total number of 3.5×10^4 HCT-116 cells was seeded in triplicates in 24-well plates. After a day, cells were co-transfected with either 10 ng empty pGL3UC vector or pGL3UC vector with circSamd4a, along with miRNA mimics using Lipofectamine 3000.

In addition, to confirm the relationship between miRNA and mRNA, the sequence of mRNA 3′ UTR was cloned into the multiple cloning sites of pGL3UC vector. A total number of 2.0×10^4 HCT-116 cells were seeded in triplicates in 24-well plates. After a day, cells were co-transfected with either 10 ng empty pGL3UC vector or pGL3UC vector with mRNA 3′ UTR sequence, along with 250 ng empty Zkscan1 vector or Zkscan1-circSamd4a vector and miRNA mimics using Lipofectamine 2000.

All luciferase constructs were verified by the Sanger sequencing before use. The miRNA mimics were transfected into the cells at a final concentration of 30 nM. The Renilla luciferase vectors were co-transfected to every sample for normalization control. The negative control siRNA and miRNA mimics were purchased from QIAGEN. Luciferase activity was detected 24 h after transfection with the dual luciferase reporter assay system (Promega), as per the manufacturer's protocol. For each individual well, firefly luciferase activity was normalized by Renilla luciferase activity.

Statistical Analysis

Data are represented as mean ± SD. Student's t test was used to analyze the results of the control and experimental samples. Results with a p value ≤ 0.05 were considered statistically significant.

SUPPLEMENTAL INFORMATION

Supplemental Information can be found online at https://doi.org/10.1016/j.omtn.2019.11.001.

AUTHOR CONTRIBUTIONS

J.R., H.K., and Y.-K.K. designed the study; J.R., D.-H.K., N.C., S.S., G.J., and Y.-H.L. conducted the study; J.R. collected data; J.R., H.K., and Y.-K.K. analyzed and interpreted data; J.R. wrote a draft of the manuscript; J.R., H.K., and Y.-K.K. revised the manuscript content; J.K., W.J.P., H.K., and Y.-K.K. acquired funding for the study.

ACKNOWLEDGMENTS

We thank our colleagues from the Department of Biochemistry and Department of Pharmacology at Chonnam National University Medical School for their valuable insight and expertise that greatly contributed to the research. This study was supported by grants from the Basic Science Research Program through the National Research Foundation of Korea (NRF), funded by the Ministry of Science, ICT & Future Planning (NRF-2018R1A2B6001104, NRF-2018R1A2B3001503, and NRF-2019R1A4A1028534). The funder has no role in study design, data collection, analysis, decision to publish, or preparation of the manuscript.

REFERENCES

1. Shanahan, C.M., Crouthamel, M.H., Kapustin, A., and Giachelli, C.M. (2011). Arterial calcification in chronic kidney disease: key roles for calcium and phosphate. Circ. Res. *109*, 697–711.
2. Mizobuchi, M., Towler, D., and Slatopolsky, E. (2009). Vascular calcification: the killer of patients with chronic kidney disease. J. Am. Soc. Nephrol. *20*, 1453–1464.
3. Wu, M., Rementer, C., and Giachelli, C.M. (2013). Vascular calcification: an update on mechanisms and challenges in treatment. Calcif. Tissue Int. *93*, 365–373.
4. Lasda, E., and Parker, R. (2014). Circular RNAs: diversity of form and function. RNA *20*, 1829–1842.
5. Hansen, T.B., Jensen, T.I., Clausen, B.H., Bramsen, J.B., Finsen, B., Damgaard, C.K., and Kjems, J. (2013). Natural RNA circles function as efficient microRNA sponges. Nature *495*, 384–388.
6. Peng, L., Yuan, X.Q., and Li, G.C. (2015). The emerging landscape of circular RNA ciRS-7 in cancer (Review). Oncol. Rep. *33*, 2669–2674.
7. Qu, S., Zhong, Y., Shang, R., Zhang, X., Song, W., Kjems, J., and Li, H. (2017). The emerging landscape of circular RNA in life processes. RNA Biol. *14*, 992–999.
8. Legnini, I., Di Timoteo, G., Rossi, F., Morlando, M., Briganti, F., Sthandier, O., Fatica, A., Santini, T., Andronache, A., Wade, M., et al. (2017). Circ-ZNF609 is a circular RNA that can be translated and functions in myogenesis. Mol. Cell *66*, 22.e9–37.e9.
9. Pamudurti, N.R., Bartok, O., Jens, M., Ashwal-Fluss, R., Stottmeister, C., Ruhe, L., Hanan, M., Wyler, E., Perez-Hernandez, D., Ramberger, E., et al. (2017). Translation of circRNAs. Mol. Cell *66*, 9.e7–21.e7.
10. Barrett, S.P., and Salzman, J. (2016). Circular RNAs: analysis, expression and potential functions. Development *143*, 1838–1847.
11. Boeckel, J.N., Jaé, N., Heumüller, A.W., Chen, W., Boon, R.A., Stellos, K., Zeiher, A.M., John, D., Uchida, S., and Dimmeler, S. (2015). Identification and characterization of hypoxia-regulated endothelial circular RNA. Circ. Res. *117*, 884–890.
12. Gruner, H., Cortés-López, M., Cooper, D.A., Bauer, M., and Miura, P. (2016). CircRNA accumulation in the aging mouse brain. Sci. Rep. *6*, 38907.
13. Sun, Y., Yang, Z., Zheng, B., Zhang, X.H., Zhang, M.L., Zhao, X.S., Zhao, H.Y., Suzuki, T., and Wen, J.K. (2017). A novel regulatory mechanism of smooth muscle α-actin expression by NRG-1/circACTA2/miR-548f-5p axis. Circ. Res. *121*, 628–635.
14. Holdt, L.M., Stahringer, A., Sass, K., Pichler, G., Kulak, N.A., Wilfert, W., Kohlmaier, A., Herbst, A., Northoff, B.H., Nicolaou, A., et al. (2016). Circular non-coding RNA ANRIL modulates ribosomal RNA maturation and atherosclerosis in humans. Nat. Commun. *7*, 12429.

15. Chen, J., Cui, L., Yuan, J., Zhang, Y., and Sang, H. (2017). Circular RNA WDR77 target FGF-2 to regulate vascular smooth muscle cells proliferation and migration by sponging miR-124. Biochem. Biophys. Res. Commun. *494*, 126–132.

16. Maass, P.G., Glažar, P., Memczak, S., Dittmar, G., Hollfinger, I., Schreyer, L., Sauer, A.V., Toka, O., Aiuti, A., Luft, F.C., and Rajewsky, N. (2017). A map of human circular RNAs in clinically relevant tissues. J. Mol. Med. (Berl.) *95*, 1179–1189.

17. Cheng, J., Metge, F., and Dieterich, C. (2016). Specific identification and quantification of circular RNAs from sequencing data. Bioinformatics *32*, 1094–1096.

18. Dobin, A., Davis, C.A., Schlesinger, F., Drenkow, J., Zaleski, C., Jha, S., Batut, P., Chaisson, M., and Gingeras, T.R. (2013). STAR: ultrafast universal RNA-seq aligner. Bioinformatics *29*, 15–21.

19. Dahl, M., Daugaard, I., Andersen, M.S., Hansen, T.B., Grønbæk, K., Kjems, J., and Kristensen, L.S. (2018). Enzyme-free digital counting of endogenous circular RNA molecules in B-cell malignancies. Lab. Invest. *98*, 1657–1669.

20. Guil, S., and Esteller, M. (2015). RNA-RNA interactions in gene regulation: the coding and noncoding players. Trends Biochem. Sci. *40*, 248–256.

21. Kramer, M.C., Liang, D., Tatomer, D.C., Gold, B., March, Z.M., Cherry, S., and Wilusz, J.E. (2015). Combinatorial control of *Drosophila* circular RNA expression by intronic repeats, hnRNPs, and SR proteins. Genes Dev. *29*, 2168–2182.

22. Wong, N., and Wang, X. (2015). miRDB: an online resource for microRNA target prediction and functional annotations. Nucleic Acids Res. *43*, D146–D152.

23. Kumar, A., Wong, A.K.L., Tizard, M.L., Moore, R.J., and Lefèvre, C. (2012). miRNA_Targets: a database for miRNA target predictions in coding and non-coding regions of mRNAs. Genomics *100*, 352–356.

24. Lewis, B.P., Burge, C.B., and Bartel, D.P. (2005). Conserved seed pairing, often flanked by adenosines, indicates that thousands of human genes are microRNA targets. Cell *120*, 15–20.

25. Jeck, W.R., Sorrentino, J.A., Wang, K., Slevin, M.K., Burd, C.E., Liu, J., Marzluff, W.F., and Sharpless, N.E. (2013). Circular RNAs are abundant, conserved, and associated with ALU repeats. RNA *19*, 141–157.

26. Rybak-Wolf, A., Stottmeister, C., Glažar, P., Jens, M., Pino, N., Giusti, S., Hanan, M., Behm, M., Bartok, O., Ashwal-Fluss, R., et al. (2015). Circular RNAs in the mammalian brain are highly abundant, conserved, and dynamically expressed. Mol. Cell *58*, 870–885.

27. Salzman, J., Chen, R.E., Olsen, M.N., Wang, P.L., and Brown, P.O. (2013). Cell-type specific features of circular RNA expression. PLoS Genet. *9*, e1003777.

28. Memczak, S., Jens, M., Elefsinioti, A., Torti, F., Krueger, J., Rybak, A., Maier, L., Mackowiak, S.D., Gregersen, L.H., Munschauer, M., et al. (2013). Circular RNAs are a large class of animal RNAs with regulatory potency. Nature *495*, 333–338.

29. Howson, J.M.M., Zhao, W., Barnes, D.R., Ho, W.K., Young, R., Paul, D.S., Waite, L.L., Freitag, D.F., Fauman, E.B., Salfati, E.L., et al. (2017). Fifteen new risk loci for coronary artery disease highlight arterial-wall-specific mechanisms. Nat. Genet. *49*, 1113–1119.

30. Martin, M., Veloso, A., Wu, J., Katrukha, E.A., and Akhmanova, A. (2018). Control of endothelial cell polarity and sprouting angiogenesis by non-centrosomal microtubules. eLife *7*, e33864.

31. Yao, Y., Jumabay, M., Ly, A., Radparvar, M., Cubberly, M.R., and Boström, K.I. (2013). A role for the endothelium in vascular calcification. Circ. Res. *113*, 495–504.

32. Meng, F., Zhao, Y., Wang, B., Li, B., Sheng, Y., Liu, M., Li, H., and Xiu, R. (2018). Endothelial cells promote calcification in aortic smooth muscle cells from spontaneously hypertensive rats. Cell. Physiol. Biochem. *49*, 2371–2381.

33. Yu, N., Erb, L., Shivaji, R., Weisman, G.A., and Seye, C.I. (2008). Binding of the P2Y2 nucleotide receptor to filamin A regulates migration of vascular smooth muscle cells. Circ. Res. *102*, 581–588.

34. Qian, S., Regan, J.N., Shelton, M.T., Hoggatt, A., Mohammad, K.S., Herring, P.B., and Seye, C.I. (2017). The $P2Y_2$ nucleotide receptor is an inhibitor of vascular calcification. Atherosclerosis *257*, 38–46.

35. Chen, X., Han, P., Zhou, T., Guo, X., Song, X., and Li, Y. (2016). circRNADb: A comprehensive database for human circular RNAs with protein-coding annotations. Sci. Rep. *6*, 34985.

36. Kwon, D.H., Eom, G.H., Ko, J.H., Shin, S., Joung, H., Choe, N., Nam, Y.S., Min, H.K., Kook, T., Yoon, S., et al. (2016). MDM2 E3 ligase-mediated ubiquitination and degradation of HDAC1 in vascular calcification. Nat. Commun. *7*, 10492.

37. Bolger, A.M., Lohse, M., and Usadel, B. (2014). Trimmomatic: a flexible trimmer for Illumina sequence data. Bioinformatics *30*, 2114–2120.

38. Kanda, Y., and Watanabe, Y. (2005). Thrombin-induced glucose transport via Src-p38 MAPK pathway in vascular smooth muscle cells. Br. J. Pharmacol. *146*, 60–67.

39. Rudich, A., Tirosh, A., Potashnik, R., Hemi, R., Kanety, H., and Bashan, N. (1998). Prolonged oxidative stress impairs insulin-induced GLUT4 translocation in 3T3-L1 adipocytes. Diabetes *47*, 1562–1569.

40. Schneider, C.A., Rasband, W.S., and Eliceiri, K.W. (2012). NIH Image to ImageJ: 25 years of image analysis. Nat. Methods *9*, 671–675.

41. Ichihara, M., Murakumo, Y., Masuda, A., Matsuura, T., Asai, N., Jijiwa, M., Ishida, M., Shinmi, J., Yatsuya, H., Qiao, S., et al. (2007). Thermodynamic instability of siRNA duplex is a prerequisite for dependable prediction of siRNA activities. Nucleic Acids Res. *35*, e123.

42. Birmingham, A., Anderson, E., Sullivan, K., Reynolds, A., Boese, Q., Leake, D., Karpilow, J., and Khvorova, A. (2007). A protocol for designing siRNAs with high functionality and specificity. Nat. Protoc. *2*, 2068–2078.

43. Kibbe, W.A. (2007). OligoCalc: an online oligonucleotide properties calculator. Nucleic Acids Res. *35*, W43–W46.